Black hole mirages: electron lensing and Berry curvature effects in inhomogeneously tilted Weyl semimetals
Submission/2210.16254v2: Reply to Reports

Andreas Haller, Suraj Hegde, Chen Xu, Christophe De Beule,
Thomas L. Schmidt and Tobias Meng

1 Report 1

1.1 The correspondence between the specific tilt profile that is the main focus of the present work and a gravitational black hole, is unclear in several ways

We thank the referee for the valuable criticism, which allowed us to improve our manuscript in several aspects, each individually addressed below.

*1.1.1 The trajectories presented in fig 1 and the effective potential presented in fig 2 contain large regions in which the semiclassical particle is *repelled* from the origin. Clearly this does not correspond to a situation with a (universally attractive) gravitational mass concentrated at the origin. The effective potential depicted in fig 2 does not contain a singularity at any point.*

The repulsion for escaping trajectories that start in the regime $\rho_t < \rho < \rho_s$ is an ubiquitous phenomenon and caused by the strong centrifugal force in the vicinity of the horizon (see, e.g., Phys. Rev. D 92, 084042). Note that for Weyl fermions ($m = 0$), the standard Newtonian term $-GMm/r$ is vanishing and only the repulsive centrifugal potential energy $\propto 1/r^2$ and the attractive cubic term contribute to the effective potential. This short discussion has been added in Sec 2.

1.1.2 the correspondence of the semiclassical trajectories to geodesic solutions of any gravitational metric is never made. Appendix A shows a recipe for finding such a correspondence in general, but does not reproduce the semiclassical trajectories in the main text (including ones accelerating away from the black hole) starting from a metric and using Einstein's equations.

To make the connection more clear, we explicitly derive the equations of motion in a plane for the Schwarzschild spacetime in Painlevé-Gullstrand coordinates and show that it exactly matches the equation for semi-classical trajectory derived in the main text.

1.1.3 No horizon is identified in the presented semiclassical dynamics or potential.

We identify and mark the analog horizon in various places, most prominently in the beginning of Sec. 3, before Sec. 3.1 and added a comment in the caption of Fig. 2 in the revised version. Furthermore, we now detail the horizon more prominently in the revised Sec. 4.

1.2 *It is not made clear in the present text how the (semiclassical and fully quantum) trajectories connect to the specific tilt profile. As the authors explain, the "horizon" in their construction coincides with the point where a type-I Weyl semimetal transitions into a type-II Weyl semimetal. At this point, the group velocity in the Weyl cone dispersion along the radial direction is zero. The fact that semiclassical trajectories transition through the horizon, and that fully quantum trajectories can even exit the horizon from the inside out, are in apparent contradiction with the naive observation of zero velocity indicating a black hole horizon. Clearly both types of behaviour must be caused by a combination of band curvature and scattering events. How this "high energy" physics enters the effective description of the (semiclassical or fully quantum) trajectories is not discussed in the present manuscript.*

In the revised version of Sec. 4 in our manuscript, we now mention explicitly that the specific tilt profiles discussed in the earlier sections are discretized on a lattice, and that we change the initial conditions by displacing the tilt center from the injecting lead by an additional parameter $\boldsymbol{r}_0$. We stress more prominently that the semiclassical trajectories in Sec. 4 are obtained by taking into account the lattice dispersion. In the revised version, we decided to neglect the Berry curvature term in the semiclassical equations of motion in Sec. 4, because it gives only small corrections to the planar movement.

The tight binding model is not axially symmetric around the z-axis, and therefore locally anisotropic. This can be investigated by a series expansion of the lattice dispersion

$$\varepsilon^{\mathrm{latt}}(\boldsymbol{k}) = \frac{v_F}{a}\sqrt{6 - 4\cos(k_y a) - 2\cos(k_x a)(2-\cos(k_y a))} \tag{1}$$

around a momentum point $\boldsymbol{\kappa}$

$$\varepsilon^{\mathrm{latt}}(\boldsymbol{k}) = \boldsymbol{v}_{\mathrm{eff}}(\boldsymbol{\kappa})\cdot(\boldsymbol{k}-\boldsymbol{\kappa}) + \varepsilon_0(\boldsymbol{\kappa}) + \mathcal{O}\left((\boldsymbol{k}-\boldsymbol{\kappa})^2\right), \tag{2}$$

where we introduced the effective velocity field

$$\boldsymbol{v}_{\mathrm{eff}}(\boldsymbol{\kappa}) = \frac{v_F^2}{a\varepsilon^{\mathrm{latt}}(\boldsymbol{\kappa})}\left(\sin(\kappa_x a)(2-\cos(\kappa_y a))\hat{\boldsymbol{e}}_x + \sin(\kappa_y a)(2-\cos(\kappa_x a))\hat{\boldsymbol{e}}_y\right). \tag{3}$$

One can confirm that $\boldsymbol{v}_{\mathrm{eff}} \approx v_F\hat{\boldsymbol{\kappa}}$ up to third order around $\kappa = 0$, and therefore $\boldsymbol{v}_{\mathrm{eff}} = v_F\hat{\boldsymbol{k}}$ everywhere around $\varepsilon^{\mathrm{latt}} = 0$. The anisotropy of the dispersion and velocity field increases towards the boundary of the Brillouin zone (see fig. 1).

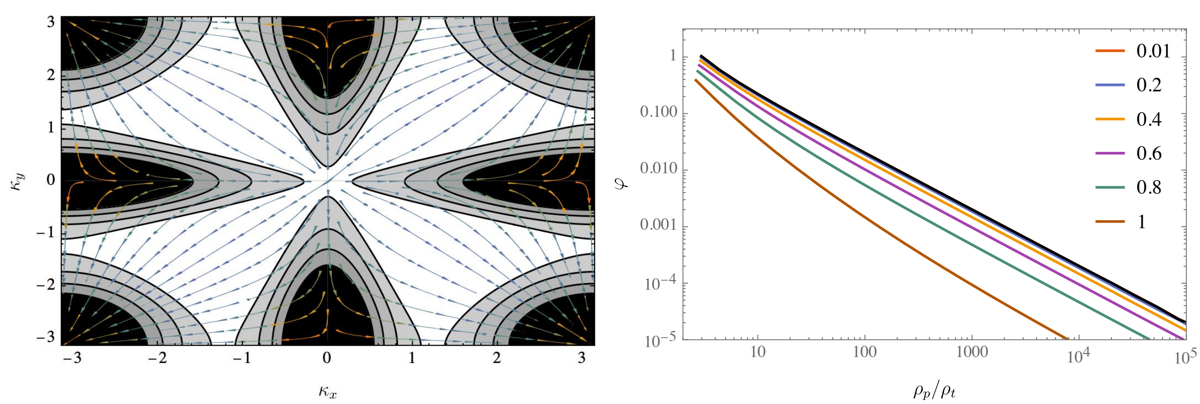

Figure 1: The left panel shows the velocity field $\boldsymbol{v}_{\mathrm{eff}}(\boldsymbol{k})$ with contour lines $v_F\,\{0.99, 0.9, 0.8, 0.7\}$ which mark the norm. In the right panel, we display the lensing angle for different initial momenta $k_x a = -k_y a$ (colored legends). The black line corresponds to the lensing angle obtained by the trajectories of the tilted isotropic linear dispersion.

For strong lensing the isotropic linear approximation can only hold if the evolution of $\boldsymbol{k}(t)$ is in the approximately isotropic region of $\boldsymbol{v}_{\mathrm{eff}}$ at low energies $\kappa \approx 0$. At larger energies and momenta $\boldsymbol{\kappa}$, the isotropic linear approximation remains valid as long as $\epsilon = |\boldsymbol{v}_{\text{eff}}(\boldsymbol{k}(t)) - v_F\hat{\boldsymbol{k}}(t)|$ is small. By comparing the deflection angle for different initial conditions, we show in fig. 1 that the trajectories obtained from the lattice dispersion show the same asymptotic decay we derived from the linear dispersion, even at high energies.

For the linear dispersion, the solutions of $\boldsymbol{v}_g(\boldsymbol{r}_t, \boldsymbol{k}) = \boldsymbol{u}(\boldsymbol{r}_t) + v_F\hat{\boldsymbol{k}} = 0$ are clearly momentum independent for a cylindrically symmetric tilt, i.e. $\boldsymbol{r}_t = \rho_t\hat{\boldsymbol{\rho}}$: particles can only enter and never leave the regime inside the horizon. Instead, for the lattice model, the condition $\boldsymbol{v}_g(\boldsymbol{r}_t, \boldsymbol{k}) = \boldsymbol{u}(\boldsymbol{r}_t) + \boldsymbol{v}_{\text{eff}}(\boldsymbol{k})$ has momentum-dependent solutions $\boldsymbol{r}_t(\boldsymbol{k})$. The horizon associated with the vanishing group velocity is thus washed out to constraints on positions that are not allowed to be crossed by specific trajectories with momentum $\boldsymbol{k}$. For axial tilt profiles, only k_z is a conserved quantity, and the constraints are thus dynamic.

To the best of our knowledge, this "meltdown" of an analog horizon has not been analyzed so far, and we include the above discussion in the revised manuscript to inspire future investigations.

1.3 *I find the discussion of a "mirage" appearing in the title and several places in the manuscript very misleading. The low-energy effective description that is argued to mimic gravitational dynamics is found to break down upon approaching the horizon. All this means however, is that the low-energy description breaks down when it is probed at short length scales or high energies. This is not surprising at all, as the low-energy description was only ever an emergent (effective) description. Saying that the emergent long-wavelength physics is a "mirage" because it disappears when probed at short (lattice) length scales, is like saying that a table is not really rigid because its rigidity disappears when probed at the atomic scale. I think this is an unfair rebranding of the already well-known limits of emergence.*

We thank the referee for bringing to our attention this important point. In short, there are several scales involved: the energy/momentum scale for linearization of the spectrum without tilt is indeed a microscopic length scale connected to the lattice constant. This length scale is entirely independent from the length scale of the tilt profile ρ_t that sets a radius at which the analogy to GR breaks down. Via the tilt profile, this length scale can easily be chosen as mesoscopic. Even in the presence of an overtilt, trajectories of particles with larger energies but far from the overtilted region are well-described by the linearized equations. Whether one sees black hole analogue physics is thus not a question of energies per se, and in this sense different from a usual "effective low-energy model"-issue. For this reason we insist that the term "mirage" is appropriate, and we believe that the criticism of the referee allowed us to significantly improve our line of reasoning in the manuscript.

In Sec. 4.1, we now discuss in more detail which trajectories can be approximated by linear dispersion semiclassics. We admit that in the previous version of our manuscript we show many cases with extreme deviations in Fig. 5, suggesting that linearization is never appropriate at high energies. We thus added new panels in Fig. 5 of the revised manuscript, which compares the deflection angle predicted by linearized and lattice dispersion semiclassics for different energy scales, clearly showing that linearization can be appropriate at high energy scales. But even if the linear description is appropriate, the semiclassical theory for the analog horizon is still doomed to fail at mesoscopic rather than microscopic distances $\rho = \rho_t \gg a$, because additional fermion doubler states become important (see, e.g. SciPost Phys. 11, 095 (2021) and Phys. Rev. Research 4). In Sec. 4.2 of our manuscript, we displace the energy level from the crossing point at $E_+^{\text{latt}} = 0$. Microscopic simulations confirm that the breakdown of (wavepacket) semiclassics in the vicinity of ρ_t occurs also for the displaced energies, even if the full lattice dispersion is taken into account. We agree with the referee that this breakdown is a priori unrelated to analog horizon physics for reasons already discussed in section 1.2 of the reply letter. However, this still allows us to draw the following conclusion: Upon approaching the tilt center, the semiclassical approximation with a linear dispersion becomes more and more inaccurate in general, and fully breaks down in the vicinity of $\rho \approx \rho_t$. Combined with the fact that electron trajectories in inhomogeneously tilted Weyl dispersion can be understood as analog gravitational lensing for certain tilt profiles, we hope we convinced the referee now that the interpretation in terms of a black hole mirage is indeed appropriate.

1.4 It is unclear at the moment why trajectories in the simulations stop at the origin, or why in section 3.2 it is mentioned that wave pakets should accumulate at the origin. From the semiclassical dynamics, the trajectories reach the origin with non-zero velocity, and there is thus no reason for them to suddenly stop there, rather than continuing, bouncing, or scattering. In the fully quantum dynamics, wave packet evolution is unitary, and accumulation at the origin is fundamentally disallowed.

The radial acceleration towards the tilt center in the Hamilton-Jacobi equation is, for our choice of tilt profiles, divergent at the tilt center. This has led us to the naive conclusion that semiclassical wave packets which cross the horizon spiral down to and accumulate at the tilt center. As is pointed out by the referee, and as we also mentioned in the previous version of the manuscript, this interpretation must be wrong. In the revised version, we decided not to mention it, and instead merely state that the semiclassical equations of motion break down close to the singularity due to a divergence of the velocity.

1.5 minor point: figure 4 appears to have a wrong title on the bottom right graph.

We thank the referee for his/her attention to detail and replaced the label of the bottom right panel.

2 Report 2

2.1 Rather than requested changes, I would propose a short discussion of the effects of impurity scattering and the related hierarchy of length scales that the system should satisfy in order to preserve/wipe out the studied effects.

We added a remark in Sec. 4.2.

3 Report 3

3.1 Contextualize further their lensing results from previous lensing proposals.

We contextualize our work in the literature of existing lensing proposals in the introduction. Our introduction already contains a large number of references from different fields of physics. We are happy to add more references, but unfortunately, without more specific instructions it is not clear to us how we should contextualize this part further.

3.2 It is not clear to me what specific phenomenon would a space dependent tilt result in that would not be possible with a space dependent fermi velocity or Weyl node separation. As the authors mention, there are previous papers that use a curved metric to interpret the results (e.g. ref. 18). I believe the manuscript would benefit from a discussion of the differentiating elements of the lenses discussed in previous works and those discussed here. In particular, is there any differentiating experiment (even if it is a gedanken experiment) when one could differentiate curved trajectories coming from space dependent tilts versus space dependent Weyl node separation?

We believe the key difference is that the eigenstates remain unaffected by the tilt profile, but they are locally changing by lensing generated from a smoothly varying inhomogeneous Fermi velocity $v_{F,i}(\boldsymbol{r})\sigma_i k_i$. For this reason, we expect that lensing proposals based on inhomogeneous Fermi velocity in general suffer from additional scattering effects that are intrinsically suppressed by lensing generated by tilt. Furthermore, a local change of eigenvectors implies that anomalous contributions from the momentum-space Berry curvature are position-dependent. As a result, the transverse motion generated from inhomogeneous Fermi velocity is entirely different from the one investigated in our manuscript. Other mechanisms that generate $\dot{\boldsymbol{k}}$ terms are mentioned in Sec. 5.

3.3 Discuss the connection with anomalous currents, if possible.

The transverse motion due to Berry curvature effects also manifest as non-equilibrium “anomalous currents” when the system is coupled to external magnetic fields and mechanical rotation. These lead to chiral magnetic and chiral vortical effects in Weyl systems, which have been studied in [1, 2, 3, 4, 5, 6, 7, 8].

References

[1] M. A. Stephanov and Y. Yin. Chiral kinetic theory. *Phys. Rev. Lett.*, 109:162001, Oct 2012.

[2] Jing-Yuan Chen, Dam T. Son, Mikhail A. Stephanov, Ho-Ung Yee, and Yi Yin. Lorentz Invariance in Chiral Kinetic Theory. *Phys. Rev. Lett.*, 113:182302, Oct 2014.

[3] Gök çe Başar, Dmitri E. Kharzeev, and Ho-Ung Yee. Triangle anomaly in weyl semimetals. *Phys. Rev. B*, 89:035142, Jan 2014.

[4] Karl Landsteiner. Anomalous transport of weyl fermions in weyl semimetals. *Phys. Rev. B*, 89:075124, Feb 2014.

[5] Maxim N. Chernodub, Alberto Cortijo, Adolfo G. Grushin, Karl Landsteiner, and María A. H. Vozmediano. Condensed matter realization of the axial magnetic effect. *Phys. Rev. B*, 89:081407, Feb 2014.

[6] Naoki Yamamoto. Photonic chiral vortical effect. *Phys. Rev. D*, 96:051902, Sep 2017.

[7] Atsuo Shitade, Kazuya Mameda, and Tomoya Hayata. Chiral vortical effect in relativistic and nonrelativistic systems. *Phys. Rev. B*, 102:205201, Nov 2020.

[8] Saber Rostamzadeh, Sevval Tasdemir, Mustafa Sarisaman, S. A. Jafari, and Mark-Oliver Goerbig. Tilt induced vortical response and mixed anomaly in inhomogeneous weyl matter. 2022.